BIOCHEMISTRY
including biophysical chemistry & molecular biology

Article

pubs.acs.org/biochemistry

Characterization of a Novel Peptide Toxin from *Acanthoscurria paulensis* Spider Venom: A Distinct Cysteine Assignment to the HWTX-II Family

Caroline B. F. Mourão,[†] Mari D. Heghinian,[‡] Eder A. Barbosa,[§] Frank Marí,[‡] Carlos Bloch, Jr.,[§] Rita Restano-Cassulini,[∥] Lourival D. Possani,[∥] and Elisabeth F. Schwartz*[,†]

[†]Laboratório de Toxinologia, Departamento de Ciências Fisiológicas, Universidade de Brasília, Brasília, DF 70910-900, Brazil

[‡]Department of Chemistry and Biochemistry, Florida Atlantic University, Boca Raton, Florida 33431, United States

[§]EMBRAPA Recursos Genéticos e Biotecnologia, Brasília, DF, Brazil

[∥]Instituto de Biotecnología, Universidad Nacional Autónoma de México, Avenida Universidad, 2001, Apartado Postal 510-3, Cuernavaca, 62210 Morelos, Mexico

Supporting Information

ABSTRACT: Spider venom toxins have raised interest in prospecting new drugs and pesticides. Nevertheless, few studies are conducted with tarantula toxins, especially with species found in Brazil. This study aims to characterize chemically and biologically the first toxin isolated from *Acanthoscurria paulensis* venom. Ap1a consists of 48 amino acid residues and has a molecular mass of 5457.79 Da. The cloned gene encodes a putative sequence of 23 amino acid residues for the signal peptide and 27 for the pro-peptide. The sequence of the mature peptide is 60−84% identical with those of toxins of the HWTX-II family. Different from the structural pattern proposed for these toxins, the disulfide pairing of Ap1a is of the ICK type motif, which is also shared by the U1-TRTX-Bs1a toxin. Ap1a induced a dose-dependent and reversible paralytic effect in *Spodoptera frugiperda* caterpillars, with an ED_{50} of 13.0 ± 4.2 μg/g 8 h after injections. In the *Drosophila melanogaster* Giant Fiber circuit, Ap1a (1.14−22.82 μg/g) reduces both the amplitude and frequency of responses from GF-TTM and GF-DLM pathways, suggesting an action at the neuromuscular junction, which is mediated by glutamatergic receptors. It is also lethal to mice (1.67 μg/g, intracranial route), inducing effects similar to those reported with intracerebroventricular administration of NMDA. Ap1a (1 μM) does not alter the response induced by acetylcholine on the rhabdomyosarcoma cell preparation and shows no significant effects on $hNa_v1.2$, $hNa_v1.4$, $hNa_v1.5$, and $hNa_v1.6$ channels. Because of its unique sequence and cysteine assignment to the HWTX-II family, Ap1a is a significant contribution to the structure−function study of this family of toxins.

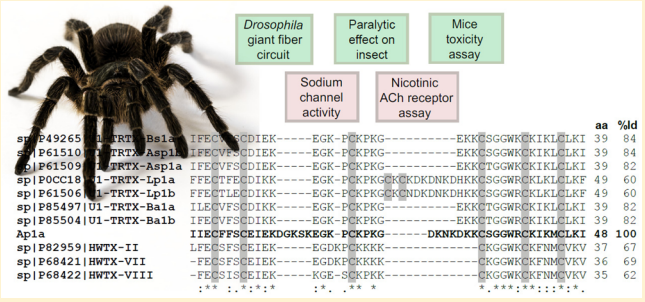

Spiders are an ancient group of arthropods and cover a wide array of ecosystems, being one of the most diverse groups of terrestrial animals.[1] Among 43678 species described to date, the Theraphosidae family (suborder Mygalomorphae) accounts for 946 species.[2] Until now, more than 200 disulfide-bridged peptides have been described from these spiders, including those predicted by transcriptomic tools,[3] this being only a fraction of the actual biochemical diversity of these animals' venoms.

Spider venom peptides can be characterized by their cysteine residue distributions along their sequences and their structural pairing.[4] Functional variability of peptides with identical sorts of frameworks and different biological activities has attracted great interest in these folds, which can be used as scaffolds for the design of compounds with desirable biological properties.

Disulfide-bridged peptides from spider venoms have two major structural motifs. The first is the inhibitory cystine knot (ICK) motif, which is characteristic of the overwhelming majority of known spider peptide toxins, with the consensual sequence C_IX_{2-7}-$C_{II}X_{3-11}$-$C_{III}X_{0-7}$-$C_{IV}X_{1-17}$-C_VX_{1-19}-C_{VI} and C_I−C_{IV}, C_{II}−C_V, and C_{III}−C_{VI} disulfide bonds, where X denotes amino acids with varying lengths.[4−6] The spatial structure of peptides with this motif is characterized by the presence of a β-hairpin and a peculiar "knot": the third disulfide bond (C_{III}−C_{VI}) pierces the ring formed by the other two disulfides and the main chain atoms joining these bonds.[4] The second is the disulfide-directed β-hairpin (DDH) motif, whose consensus sequence proposed by Wang and collaborators[7] is $CX_{5-19}CX_2$(G or P)$X_2CX_{6-19}C$. This motif does not have the cysteine knot and includes an antiparallel β-hairpin stabilized by only two mandatory disulfide bonds, the two that make up

Received: January 1, 2013
Revised: March 14, 2013
Published: March 15, 2013

   dx.doi.org/10.1021/bi4000035 | *Biochemistry* 2013, 52, 2440−2452

most of the hydrophobic core. Thus, loop 1 is no longer necessarily connected to the N-terminal cysteine such as in the ICK motif, and loop 3 usually has five amino acid residues with a central Gly or Pro to ensure stability prior to the first β-strand. The DDH motif is found in proteins from diverse organisms, except Archaea and Eubacteria, suggesting that this structural motif would have evolved in an ancestral eukaryote prior to the divergence of plants, animals, and fungi. Depending on the position of an additional disulfide bridge, the DDH motif can generate an ICK motif, thus suggesting that the ICK fold would be a molecular evolution of the DDH fold.[7] Recently, the first superfamily of Kunitz-type toxins from spiders was reported. The Kunitz-type motif usually has a polypeptide chain of ~60 amino acid residues and three disulfide bridges with a C_I−C_{VI}, C_{II}−C_{IV}, and C_{III}−C_V bonding pattern. These peptides are found in various venomous animals, and besides serine protease inhibition, some of them also block ion channels, mainly voltage-gated potassium channels.[8]

Another structural scaffold in tarantula venom toxins was demonstrated by determining the structure of huwentoxin-II (HWTX-II or U1-TRTX-Hh1a), isolated from *Haplopelma schmidti* venom, with a different disulfide pairing (C_I−C_{III}, C_{II}−C_V, and C_{IV}−C_{VI}).[9] The HWTX-II structure does not present the cysteine knot and has been defined as a DDH scaffold,[10] although it may be considered as an evolution of the basic DDH motif as defined by Wang and collaborators.[7] It has been suggested that because of the high degree of sequence similarity between toxins of the HWTX-II family, they would probably adopt the DDH fold.[10−12]

Here we present the chemical and biological characterization of Ap1a, the first peptide isolated from the venom of the Brazilian spider *Acanthoscurria paulensis*, with activity in both insects and mammals possibly affecting glutamate neurotransmission and with a different cysteine arrangement for the HWTX-II family.

EXPERIMENTAL PROCEDURES

Animals and Permits. Male and female adult specimens of *A. paulensis* were collected at various locations of Distrito Federal, in Brazil, under Instituto Chico Mendes de Conservação da Biodiversidade (ICMBio) license 24227-1. They were kept alive in the laboratory at the University of Brasília in individual terrariums and fed fortnightly with cockroaches and received water *ad libitum*. Animals were contained in accordance with the ethical guidelines of the Brazilian Society for Neuroscience and Behavior, which follows the guidelines for animal care prepared by the Committee on the Care and Use of Laboratory Animal Resources of the National Research Council (Washington, DC). The number of animals was kept to the minimum necessary to test the concept.

Purification Procedures. A pool of venom from 15 male and female *A. paulensis* spiders was obtained monthly and fractionated as described previously.[13] The fraction that eluted at 41.0% acetonitrile (named Ap1a) was collected, vacuum-dried, and rechromatographed by high-performance liquid chromatography (HPLC) through a C18 reversed phase analytical column (Synergi 4 μm Fusion-RP 80 Å, 250 mm × 4.60 mm, Phenomenex) with a water gradient (0.12% trifluoroacetic acid, which is solvent A) and acetonitrile (0.10% TFA, which is solvent B). The peptide was purified using two subsequent steps of chromatography with the same equipment and column with optimized gradients, with the final gradient shown in the legend of Figure 2B. Samples were dried under vacuum and stored at −20 °C. The peptide was quantified by the absorbance at 280 nm.[14]

Mass Spectrometry Analysis. The molecular mass and purity of peptide Ap1a were determined on an UltraFlexIII matrix-assisted laser desorption ionization time-of-flight (MALDI-TOF/TOF) mass spectrometer (Bruker Daltonics) in the reflected and linear positive modes, as previously described.[13] In addition to MALDI-TOF/TOF MS, some fragments generated after digestion with pepsin and trypsin were also analyzed in a micrOTOF-Q II mass spectrometer (Bruker Daltonics) equipped with an orthogonal electrospray ionization source (ESI) operated in the positive mode. Samples were diluted in variable concentrations of 1% formic acid in a water/acetonitrile mixture (1:1, v:v) and applied to the mass spectrometer source by direct infusion.

Amino Acid Sequence Determination. The N-terminal amino acid sequence of peptide Ap1a was determined by the automated Edman degradation method on a Beckman (Palo Alto, CA) LF 3000 protein peptide sequencer. Additionally, MS/MS sequencing was performed with the chromatographic fractions obtained after reduction, alkylation, and digestion of Ap1a using the UltraFlexIII MALDI-TOF/TOF mass spectrometer (Bruker Daltonics) in the LIFT mode.[15] Briefly, an aliquot of 50 μg of the native Ap1a was reduced with 25 mM dithiothreitol (DTT) in 50 mM ammonium carbonate buffer and incubated at 60 °C for 60 min under constant agitation. After reduction, the sample was alkylated with 25 mM iodoacetamide in 50 mM ammonium carbonate buffer and incubated for 40 min under the conditions described above and under light protection. The alkylated sample was digested with Glu-C endopeptidase (Sigma-Aldrich) for 60 min at 37 °C under constant agitation, with an enzyme:substrate ratio of 1:25 (v:v).

The digests were fractionated in an UFLC system using a Shim-pack XR-ODS analytical column (Shimadzu, 30 mm × 2.0 mm, 2.2 μm), with a flow rate of 0.4 mL/min and detection at 216 and 280 nm. The following binary gradient was used: 5% solution B for 5 min, 5 to 50% B for 20 min, 60 to 90% B for 2 min, and 90% B for 3 min. Subfractions were manually collected, vacuum-dried, and stored at −20 °C until they were used. After chromatography, the subfractions were submitted to mass spectrometry analysis (the MS/MS spectra were analyzed manually).

Similarity searches were performed using blastp (http://www.ncbi.nlm.nih.gov/blast) and Fasta3 (http://www.ebi.ac.uk/fasta) with an *e* value cutoff set to $<10^{-5}$ to identify putative functions. ClustalW version 2.0[16] was used for sequence alignments, comparison of the amino acid substitutions, and calculation of the identity percentage between paired sequences.

Construction of the cDNA Library and Gene Cloning. A cDNA library was constructed from total RNA obtained from *A. paulensis* venom glands, which were dissected from one male spider 4 days after venom extraction by electrical stimulation. The total RNA was extracted using the ZR-Duet DNA/RNA Miniprep kit (Zymo Research). The full-length cDNA library was prepared by means of the In-Fusion SMARTer cDNA Library Construction kit (Clontech Laboratories, Palo Alto, CA), according to the long-distance polymerase chain reaction (PCR) protocol. The cDNA inserts were cloned into linearized pSMART2IF plasmids. The recombinant plasmids were transformed into electrocompetent *Escherichia coli* DH5α cells. The forward and reverse screening primers (10 μM)

dx.doi.org/10.1021/bi4000035 | *Biochemistry* 2013, 52, 2440−2452

from the Advantage 2 PCR kit (Clontech Laboratories) were used for the PCR of the cDNA library. Selected plasmids with >300 bp cDNAs were isolated using the alkaline lysis method, and single-pass sequencing of the 5′-termini was conducted with the M13 forward primer (5′-TGT AAA ACG ACG GCC AGT-3′) using an automatic sequencer (ABI 3130 XL genetic analyzer, Applied Biosystems), according to the manufacturer's instructions. The bioinformatics analyses were performed as previously described.[17] The protein and nucleotide sequence data reported in this paper are deposited in UniProt Knowledgebase as entry B3EWY4.

Assignment of Disulfide Bonds. Immobilized pepsin (Pierce, Rockford, IL) was added to 100 μg of native peptide, which was digested for 90 min at 37 °C, under constant agitation and according to the manufacturer's instructions. Then, the sample was centrifuged (5000*g* for 5 min), and the supernatant was submitted to HPLC fractionation in a C18 reversed phase analytical column (Synergi 4 μm Fusion-RP 80 Å, 250 mm × 4.60 mm, Phenomenex) at a flow rate of 1.0 mL/min and monitored at 216 and 280 nm. A linear gradient from 0 to 60% solution B for 60 min was used. The chromatographic fractions had their molecular masses analyzed by MALDI-TOF/TOF MS. The two major fractions (P1 and P2) were also analyzed by micrOTOF-Q II MS.

The P1 fraction was vacuum-dried and digested with immobilized trypsin (Pierce) according to the manufacturer's instructions. The reaction was allowed to run for 9 h at 37 °C, under constant agitation. The sample was then centrifuged (5000*g* for 5 min), and the supernatant was submitted to UFLC fractionation in a Shim-pack XR-ODS analytical C18 column as described in Amino Acid Sequence Determination. The molecular masses and amino acid sequences of the chromatographic fractions were analyzed by MALDI-TOF/TOF MS (MS and MS/MS modes) and micrOTOF-Q II. The fractions containing ions corresponding to tryptic fragments with single disulfide bonds were subsequently reduced with 10 mM dithiothreitol (DTT) in 10 mM ammonium carbonate buffer and maintained for 30 min at 60 °C. Then, the reduced fractions were analyzed by MALDI-TOF/TOF MS (MS and MS/MS modes).

The enzymes were chosen on the basis of the prediction of potential cleavage sites of Ap1a by the enzymes pepsin (at pH >2) and trypsin using PeptideCutter (http://web.expasy.org/peptide_cutter/), leaving a single Cys residue at each distinct fragment.

Secondary Structure Prediction. The prediction of Ap1a secondary structure was performed by the tool available on the PSIPRED server (http://bioinf.cs.ucl.ac.uk/psipred/).

Paralytic Effect on Insects. The paralyzing activity of Ap1a toxin was assayed on *Spodoptera frugiperda* larvae (Lepidoptera, Noctuidae) weighing on average 100 mg each. The peptide was dissolved in deionized water, and the tests consisted of injecting 2 μL of four different peptide doses (10, 15, 25, and 50 μg/g of animal) into the ventro-posterior region of the larvae, between the penultimate and last pair of legs (n = 10 per group). Control animals (n = 15) received 2 μL of water through the same route of administration. The larvae were individually kept in transparent plastic containers and monitored at regular time intervals (1, 3, 5, 8, 12, 24, and 48 h after the injection) for signs of paralysis or death. For determination of the mean effective dose (ED_{50}) that paralyzes 50% of the animals, both partial and total paralysis were considered (partial paralysis affected locomotion by paralyzing only the rear half of the larvae) during the 8 h experiment. ED_{50} values and respective confidence indices were calculated using the Probit method[18] and BioStat 2009.

***Drosophila* Giant Fiber Circuit.** The effects of Ap1a were observed on the *Drosophila melanogaster* giant fiber system (GFS), a well-characterized neuronal circuit (see Figure 5A) composed of cholinergic synapses, electrical connections (GAP junctions), and glutamatergic neuromuscular junctions (NMJs).[19,20] For this assay, picomolar amounts of the compound were injected into the living flies (1.1 ± 0.1 mg weight) while simultaneously obtaining electrophysiological recordings, as previously described.[19]

The frequency and amplitude of responses were calculated as percentages and compared to the average of train responses before peptide injection and to control flies injected with 46 nL of a 0.7% saline solution[21] in deionized water (n = 10). Statistical analyses of the frequency and amplitude values of both GF-DLM and GF-TTM pathways were performed by two-way analysis of variance (ANOVA) followed by a Bonferroni post-test, comparing the values obtained at each time of each dose with the equivalent time of the control group (saline).

For Ap1a toxin injection, flies were injected with 46 nL of the peptide diluted in an insect saline solution at four different doses: 5, 25, 50, and 100 μM, the equivalent of 1.14, 5.71, 11.41, and 22.82 ng/mg, respectively (or 0.21, 1.05, 2.10, and 4.18 pmol/mg, respectively) (n = 8 ± 2 each). The responses from GF-TTM and GF-DLM pathways were tested with 10 sweeps of 10 stimulus trains at 10 Hz before and after the injection, immediately after the 1 Hz stimulation period (1 min) and 5, 10, and 15 min later.

Nicotinic Acetylcholine Receptor Assay (nAChR). The physiological activity of Ap1a was also performed by patch clamp using the muscular nAChR assay in the rhabdomyosarcoma TE671 cell line, as previously described.[22] Currents were elicited by applying 10 μM ACh for 4−6 s at least thrice at intervals of 90 s. Then, Ap1a was applied at a concentration of 1 μM for 1 min, followed by ACh addition. The α-bungarotoxin (0.1 μM) was used as a positive control. Data were analyzed off-line by using pClamp9 and Origin7 (Microcal).

Mice Toxicity Assay. The toxicity to mammals of the Ap1a toxin was tested by intracranial injections (with the aid of a 10 μL Hamilton syringe) in male Swiss albino mice (*Mus musculus*) with an 18 g body weight. The experimental group (n = 3) received a unique dose of 30 μg of Ap1a per animal (the equivalent of 1.67 μg/g), in a total volume of 2 μL of the peptide solubilized in deionized water. The control group (n = 3) was injected with 2 μL of deionized water each. The toxic effects of the peptide were analyzed by descriptive statistics, comparing the behavioral and physiological changes between experimental and control group during the first hour of the experiment. At the end, the surviving animals were euthanized with an overdose of sodium pentobarbital (~75 mg/kg).

Sodium Channel Activity. HEK293 cell lines stably expressing human $Na_v1.2$, $Na_v1.4$, $Na_v1.5$, and $Na_v1.6$ were used to measure Ap1a activity on sodium channels as previously reported.[23] Ap1a was diluted in the extracellular solution from a stock solution in water, to a final concentration of 1 μM. Currents were elicited by pulses (200 ms) from a holding potential of −120 mV until a value of −10 mV was reached, preceded by a prepulse of 5 ms at 50 mV, followed by depolarization (50 ms) at −10 mV. Data were analyzed off-line

by using Clampfit10 (Molecular Devices) and Origin7 (Microcal).

Figure 1 summarizes the strategy used in this study to perform the chemical and biological characterization of the Ap1a toxin.

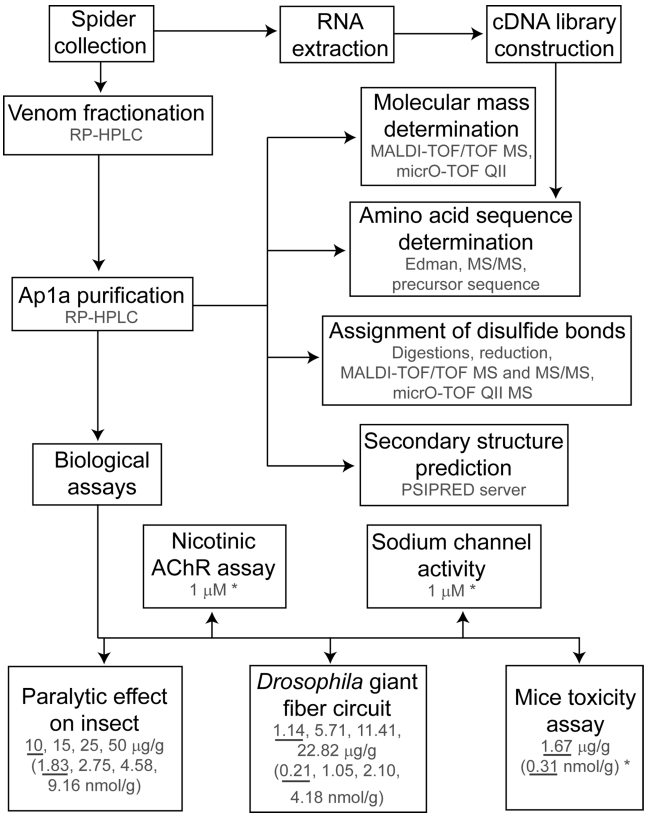

Figure 1. Experimental strategy used to perform the chemical and biological characterization of the Ap1a toxin. The scheme presents a comparison of the doses used in the biological assays, showing the smallest assayed doses that presented significant effects (underlined). In the assays marked with asterisks, only one toxin concentration was tested.

RESULTS

Chromatographic Separation and Mass Spectrometry. The chromatographic fraction that eluted at 51.0 min (41% acetonitrile) during whole venom fractionation (Figure 2A) went through two additional purification steps by RP-HPLC, until the pure peptide named Ap1a was obtained (Figure 2B), the first peptide characterized from *A. paulensis* venom. It corresponds to approximately 8% of the total venom (calculation performed with regard to the area under curve in whole venom chromatography at 216 nm). Its molecular mass determined by micrOTOF-Q II MS was $[M + 6H]^{6+}$ = 910.465 Da, which is equivalent to the monoisotopic molecular mass of 5457.79 Da (Figure 2C).

Amino Acid Sequencing and Similarities. The determination of the primary structure of Ap1a was performed by complementary strategies (Figure 2D). From the 48 amino acid residues that make up the peptide, the first 18 residues were originally determined by Edman degradation.

After reduction and alkylation, Ap1a was subjected to partial digestion with Glu-C endopeptidase, from which two ions were identified by MALDI-TOF/TOF MS: m/z 2104.97 and 3548.48. These two ions were submitted to MS/MS analysis, allowing the identification of the sequence from residue Ile1 to Trp38.

The interpretation of the spectrum generated by fragmentation of the ion at m/z 2104.97 coincided with the first 18 residues of the N-terminal region previously obtained by Edman degradation (data not shown). The theoretical monoisotopic molecular mass ($[M + H]^+$) of this peptide fragment (Ile1−Glu18), considering the reduced and non-alkylated cysteine residues, is equal to 2104.99 Da, which is very close to the molecular mass obtained experimentally, indicating that there was no alkylation on these two cysteine residues (C_I and C_{II}). With the exception of this fragment, all other *de novo* sequences and differentiation of isobaric residues was carried out *a posteriori*, based on the Ap1a precursor sequence.

The fragmentation spectrum of the second ion generated by digestion with Glu-C (m/z 3548.48) was also analyzed, and the GKP**C**KPKGDKNKDKK**C**SGGW partial sequence was obtained, with two alkylated cysteines (C_{III} and C_{IV}) (data not shown). The data obtained were not sufficient to interpret the whole spectrum, with 1273.12 Da missing from both y-ion series (excluding 19 Da corresponding to the sum of the water molecule and the ionization proton) and b-ion series for completion of the sequence. However, after obtaining the complete peptide sequence by the precursor nucleotide sequence, we observed that the value for the sum of amino acid residues that make up the remaining C-terminal fragment (R**C**KIKM**C**LKI) is equal to 1216.71 Da. The obtained value of 1273.71 Da for the noninterpreted spectrum sector indicated that only one cysteine residue located in this fragment was alkylated.

The complete peptide sequence was subsequently deduced by transcriptomic analysis (Figure 2D), performed after construction of the cDNA library from *A. paulensis* venom glands, which allowed the cloning of the Ap1a precursor. This precursor presented 297 nucleotides that encode a 98-amino acid residue peptide (see Figure S1A of the Supporting Information), including a signal peptide of 23 amino acid residues, a pro-peptide with 27 residues, and a mature segment with 48 residues, whose theoretical molecular mass ($[M + H]^+$ = 5457.77 Da) was equal to the Ap1a experimental molecular mass ($[M + H]^+$ = 5457.79 Da).

At least seven putative sequences available in public databases were 55−74% identical with the Ap1a precursor sequence (Figure S1A of the Supporting Information). U1-TRTX-Lsp1b (LTx2), U1-TRTX-Lsp1a (LTx1), and U1-TRTX- Lsp1c (LTx3), from the tarantula *Lasiodora* sp., showed the highest levels of identity, 74, 72, and 68%, respectively. U3-TRTX-Cj1b (JZTX-47), from the spider *Chilobrachys jingzhao*, had the lowest value (55%), while the other Huwentoxin putative sequences were 60% identical with the Ap1a precursor. Considering only the signal peptide and the pro-peptide sequences, the similarity of Ap1a was higher with sequences of *Lasiodora* sp., with 73−91% identity with regard to signal peptides and 74−78% with regard to pro-peptides. The other putative sequences used in this alignment were 50−56% identical in the region of the signal peptide and 28−46% identical in the pro-peptide segment.

The Ap1a mature peptide is similar with toxins belonging to the HWTX-II family (Figure S1B of the Supporting Information), which were all isolated from the venom of Theraphosidae spiders. Toxins U1-TRTX-Lp1a and U1-TRTX-Lp1b, from *Lasiodora* sp., showed the lowest percentage of

dx.doi.org/10.1021/bi4000035 | *Biochemistry* 2013, 52, 2440−2452

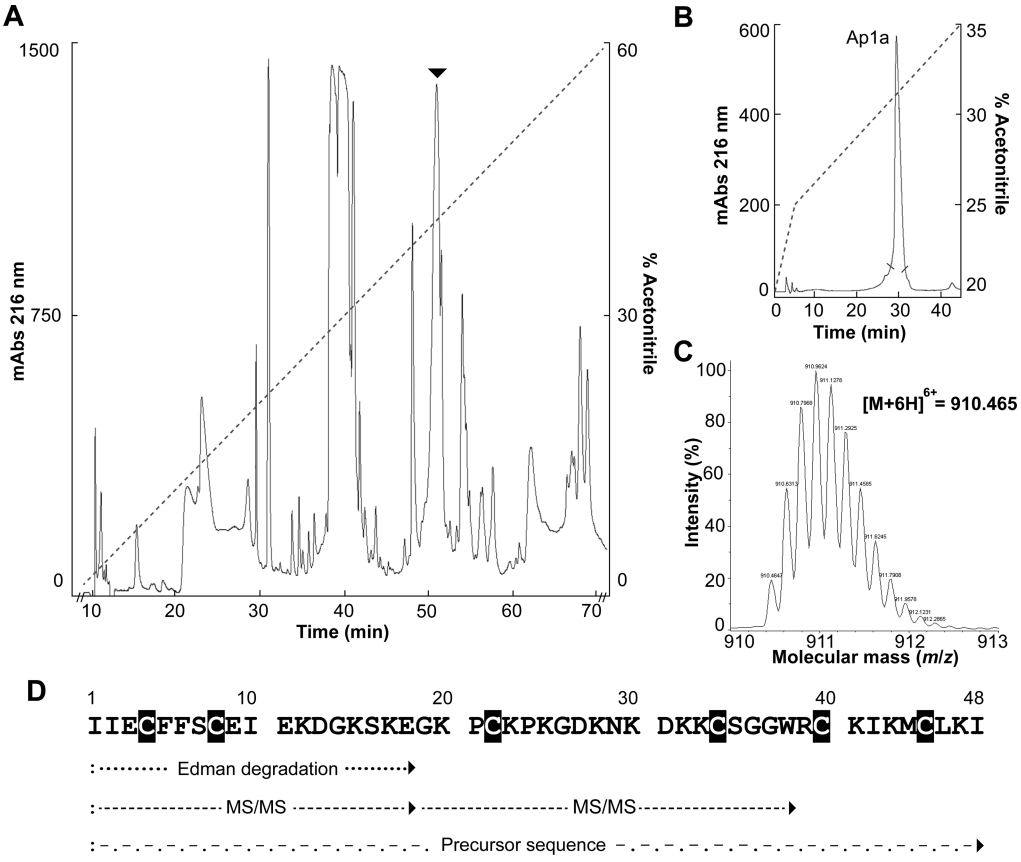

Figure 2. (A) RP-HPLC fractionation of 5.0 mg of *A. paulensis* soluble venom. Fractionation in a C18 semipreparative column (Phenomenex) using a gradient of acetonitrile (ACN) that is represented by the dashed line, with a flow rate of 1 mL/min and absorbance at 216 nm. The component labeled with the arrow corresponds to an elution time of 51.0 min (41% ACN) and was used for further purification. (B) Rechromatography of the component that eluted at 51.0 min using a C18 reversed phase analytical column, eluted with a gradient from 20 to 25% B from 0 to 5 min and from 25 to 32% B from 5 to 45 min, at a rate of 1 mL/min, as indicated by the dashed line. The two traces at the peak base indicate the beginning and end of fraction collection. (C) Mass spectrometry analysis of Ap1a by micrOTOF-Q II, presenting the monoisotopic distribution of the +6 charged ion. (D) Primary sequence of Ap1a. The first 18 amino acid residues in the N-terminal region were obtained by automated Edman degradation. The amino acid residues of positions 1−18 and 19−38 were obtained by MS/MS sequencing after reduction, alkylation, and digestion with Glu-C endopeptidase. Only a partial sequence (residues 19−38) was obtained from the second digest fragment (residues 19−48). The complete amino acid sequence was determined by transcriptomic analysis.

A

Sequence*	MM (*m/z*)		MM after reduction (*m/z*)		Disulfide bond
	Theoretical	Experimental**	Theoretical	Experimental*	
IIE**C**F | **C**SGGWR	1,286.56	1,286.57	C_I: 624.30 C_{IV}: 665.28	C_I: 624.29 C_{IV}: 665.27	C_I-C_{IV}
FS**C**EIEK | **C**K	1,102.49	1,102.49	C_{II}: 855.39 C_V: 250.12	C_{II}: 855.37 C_V: –	C_{II}-C_V
EGKP**C**KPK | M**C**LK	1,377.70	1,377.70	C_{III}: 886.48 C_{VI}: 494.25	C_{III}: – C_{VI}: –	C_{III}-C_{VI}

B

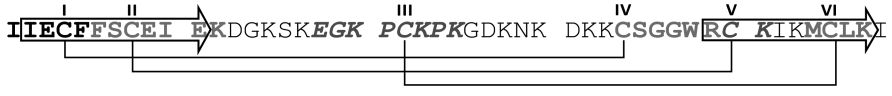

Figure 3. Assignment of disulfide bonds of Ap1a. (A) Amino acid sequences and molecular masses (MM) of ions generated after digestion with pepsin and trypsin, and after reduction. The ions obtained after reduction are indicated by the number of the Cys (C_I−C_{VI}) present in their sequences. One asterisk denotes MALDI-TOF/TOF MS. Two asterisks denote micrOTOF-Q II. A dash denotes undetected MM. (B) Global view of Ap1a disulfide bonds and predicted secondary structure. The Cys residues are designated by Roman numerals. In bold black letters are shown the fragments obtained after pepsin digestion of the native peptide. In bold gray letters are shown the fragments obtained after trypsin digestion. The amino acid residues predicted to form the two strands of the β-sheet structure are shown inside the arrows.

identity (60%) with Ap1a. The HWTX-II, the prototype member of this peptide family, also showed a moderate identity percentage (67%). The highest identity percentages were with toxins U1-TRTX-Bs1a (84%), U1-TRTX-Asp1b (84%), U1-

dx.doi.org/10.1021/bi4000035 | *Biochemistry* 2013, 52, 2440−2452

TRTX-Asp1a (82%), U1-TRTX-Ba1a (82%), and U1-TRTX-Ba1b (82%).

Assignment of Disulfide Bonds. Ap1a cysteine pairing was assessed by peptide digestion with pepsin and trypsin, followed by mass spectrometry analysis (MS and MS/MS).

After digestion with pepsin and RP-HPLC fractionation, two main fractions were obtained. The first fraction (P1), which referred to the digested peptide form, had $[M + H]^+$ = 5475.80 Da ($[M + 7H]^{7+}$ = 783.115 Da), and the second fraction (P2), which was the peptide in its native form, had $[M + H]$ = 5457.75 Da ($[M + 7H]^{7+}$ = 780.536 Da) (data not shown). The 18.0 Da difference between these two forms was due to the addition of a water molecule after a single peptide bond cleavage, with no amino acid residue or peptide fragment loss, suggesting that a cysteine bond linked the two fragments. According to the putative pepsin cleavage sites, it was expected that cleavage had occurred at the peptide's N-terminal region, forming the IIEC, IIECF, or IIECFF fragment.

The digested peptide fraction was further treated with trypsin and fractionated in an UFLC system (data not shown). The tryptic digests had their molecular masses analyzed via micrOTOF-Q II and MALDI-TOF/TOF MS. The latter equipment was also used to perform MS/MS sequencing (Figure 3A).

The interpretation of the fragmentation spectrum of the ion at m/z 1286.57 (m/z 1286.57 via micrOTOF Q-II or m/z 1286.52 via MALDI-TOF/TOF MS) yielded the sequences IIECF and CSGGWR (Figure S2A of the Supporting Information), corresponding to the C_I–C_{IV} linkage. The fragment containing the ion with the linked cysteines was also found (CCSGGW). After DTT reduction of this fragment, the two ions responsible for the C_I–C_{IV} disulfide pair (m/z 624.29 and 665.27) (Figure 3A) were detected. Fragmentation of both precursor ions confirmed the IIECF (C_I) and CSGGWR (C_{IV}) sequences (Figure S2B,C of the Supporting Information).

A second ion, at m/z 1102.49, was also identified in one of the chromatographic fractions after trypsin digestion. Its experimental molecular mass was equal to the theoretical molecular mass of the fragment containing the C_{II}–C_V linkage (Figure 3A), which was confirmed by MS/MS sequencing (Figure S3A of the Supporting Information). The sequence FSCEIEK, containing residue C_{II}, was observed in the y-ion series. The sequencing of the C_{II}–C_V binding fragment yielded a FSCCK ion, which together with the EIEK ion completes the sequence of the $[M + H]^+$ = 1102.49 Da fragment (FSCEIEK/CK). The 247.04 Da difference is due to a mass difference of the CK fragment plus 18 Da of the water molecule, minus 1 Da from the H^+ gain of the cysteine present in the sequenced fragment (KEIECSF) (102.15 Da + 128.17 Da + 18 Da − 1 Da = 247.32 Da). After reduction of the $[M + H]^+$ = 1102.49 Da fragment, the ion at m/z 885.37 was detected. It contains residue C_{II} (Figure 3A) and the sequence FSCEIEK (Figure S3B of the Supporting Information).

The third ion obtained after digestion of the Ap1a toxin with pepsin and trypsin was that at m/z 1377.70, which was shown to contain the C_{III}–C_{VI} linkage (Figure 3A) and the sequence EGKPCKPK/MCLK (Figure S4A of the Supporting Information). The main series of fragments of this precursor ion are shown in Figure S4B of the Supporting Information. In the top part of the spectrum, the b-ion series containing C_{III} is shown (EGKPCKPK), and below it, the y-ion series of the sequence with the cysteine binding is shown (KLCCPKGE) (Figure S4B-b of the Supporting Information). The 502.15 Da difference corresponds to the sum of the molecular masses of the amino acid residues not contained in this product ion (M/KPK) plus 18 Da of the water molecule due to peptide bond cleavage.

The ions corresponding to the KLCC/M fragment were also detected in the y-ion series (Figure S4B-c of the Supporting Information), containing the cystine bond (in Figure S4A of the Supporting Information, it is shown as the Met residue immediately below the KLCC series, on the left). The ions corresponding to residues EGKP complementary to this fragmentation were sequenced in the y-ion series (Figure S4A of the Supporting Information, top right). Other ions produced by the fragmentation formed the KLCCP/M series (Figure S4B-d of the Supporting Information), with the methionine chemically linked to cysteine C_{VI} (in Figure S4A of the Supporting Information, this Met residue is on the bottom right of the y-ion series KLCCP). Another fragmentation spectrum has led to the KLCCPKGE/M ion series (Figure S4B-e of the Supporting Information). In Figure S4A of the Supporting Information, this Met residue is on the bottom right of the y-ion series KLCCPKGE. The remaining amino acid residues to complete the sequence of the precursor ion of all these series (KPK, M/KPK, and LK) were also detected and are shown in Figure S4A of the Supporting Information.

Figure 3B summarizes the results of the determination of the three disulfide bonds of Ap1a, which exhibits the following cysteine pairing pattern: C_I–C_{IV}, C_{II}–C_V, and C_{III}–C_{VI}.

Secondary Structure Prediction. The Ile2–Glu11 and Arg39–Lys47 amino acid segments of Ap1a were predicted to form a double-stranded β-sheet structure (Figure 3B). The two predicted strands are connected by the C_{II}–C_V disulfide bond.

Paralytic Effect on Insects. The Ap1a peptide induced paralysis in *S. frugiperda* larvae at all tested doses, in a dose-dependent manner. The median effective dose (ED_{50}) was found to be 13.01 ± 4.21 μg/g (5.35–18.64) (Figure 4),

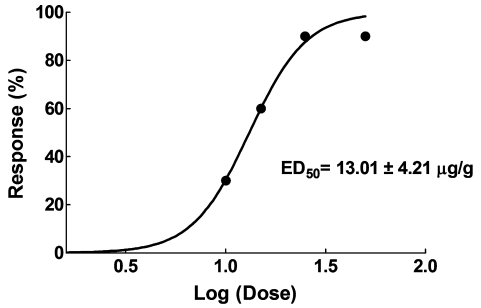

Figure 4. Dose–response curve obtained from intraperitoneal injection of *A. paulensis* venom into *S. frugiperda* larvae. R^2 = 0.9878.

equivalent to 2.38 ± 0.77 nmol/g. At all assayed doses, the greatest percentages of paralysis were observed 8 h after the peptide had been administered, which was the chosen time for the ED_{50} determination. After this time, the effect was reversible in most larvae. However, 20–30% of cases in each dose remained paralyzed until the end of the experiment (48 h), with partial paralysis at the two smallest doses (10 and 15 μg/g) and total paralysis at the two largest ones (25 and 50 μg/g). The paralytic effect began 15 min after injection at the largest dose, and at the two smallest doses, this time was extended to 5–8 h. At the largest dose, the paralytic effect was more noticeable than at others; however, the maximal effect percentage of this dose was equal to the dose of 25 μg/g, both

dx.doi.org/10.1021/bi4000035 | *Biochemistry* 2013, 52, 2440–2452

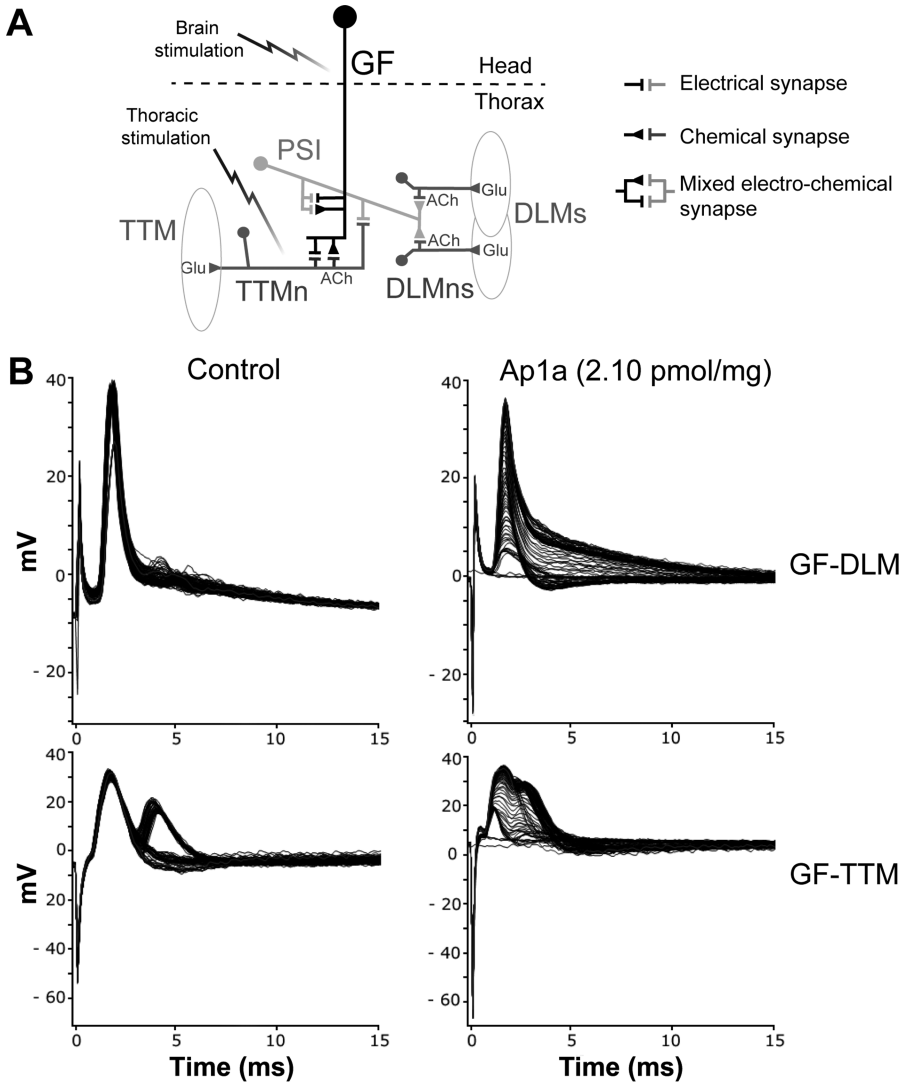

Figure 5. *Drosophila* giant fiber (GF) system and records of Ap1a injection. (A) Schematic indicating the neurons and known synaptic connections of the GFS, with only one-half of the bilateral circuit shown. In this circuit, each bilateral GF extends from the brain to the thoracic ganglion, where it forms an electrochemical synapse to the tergotrochanteral motor neuron (TTMn), which innervates the tergotrochanteral muscle (TTM). It also makes an electrochemical synapse to the peripherally synapsing interneuron (PSI), which makes cholinergic chemical synapses to the dorsal longitudinal motor neurons (DLMns) that, in turn, innervate the dorsal longitudinal muscles (DLMs). PSI and TTMn are also coupled via electrical synapses. Adapted from ref 40. (B) Response traces of GF-DLM (top) and GF-TTM (bottom) to single pulses given at 1 Hz just before, during, and continuing after injections for a total of 100 sweeps, for monitoring any immediate effects after compound injection on the function of the GF system. Records were obtained with injections of saline (n = 10, control group, left) and Ap1a (n = 8 ± 2, right).

causing paralysis in 90% of tested larvae. Larger doses were not used because of the limited amount of isolated peptide. However, because Ap1a showed a dose-dependent effect and considering that paralysis had a long duration for the largest dose, it is expected that larger doses are lethal to the larvae.

***Drosophila* Giant Fiber Circuit.** To test the effect of Ap1a in the *D. melanogaster* giant fiber (GF) circuit (Figure 5A), four different peptide doses were injected into the flies (n = 8 ± 2). The effects on DLM and TTM responses were recorded and compared with those from flies injected with saline (n = 10).

The response latency (defined as the time between brain stimulation and muscle depolarization) was consistent with the expected responses for a wild-type fly (between 1.3 and 1.7 ms for the GF-DLM pathway and between 0.7 and 1.2 ms for GF-TTM pathway), indicating a healthy preparation and appropriate recording techniques.[24] The "frequency of following" after 10 sweeps of 10 stimulus trains at 100 Hz before the saline or peptide injection was also observed, with a 1:1 proportion for both pathways. Only flies with a response frequency equal to 100 ± 2% were selected to continue the experiment.

During peptide injection, at the monitoring period with 100 pulses at 1 Hz, a reduction in the amplitude of both pathways' response in comparison to the control group was observed (Figure 5B).

This reduction in amplitude was also observed for both pathways during the period of 10 sweeps of 10 stimulus trains at 100 Hz (with 1 s between each sweep), immediately after peptide injection (1 min), and then 5, 10, and 15 min after that (Figure 6A,B). Statistical analysis performed by two-way ANOVA followed by a Bonferroni post-test indicated significant differences between doses, times, and time−dose interactions with $p < 0.001$ in the results relative to the amplitude of responses of GF-DLM [dose, $F_{(4, 42)}$ = 61.88;

dx.doi.org/10.1021/bi4000035 | *Biochemistry* 2013, 52, 2440−2452

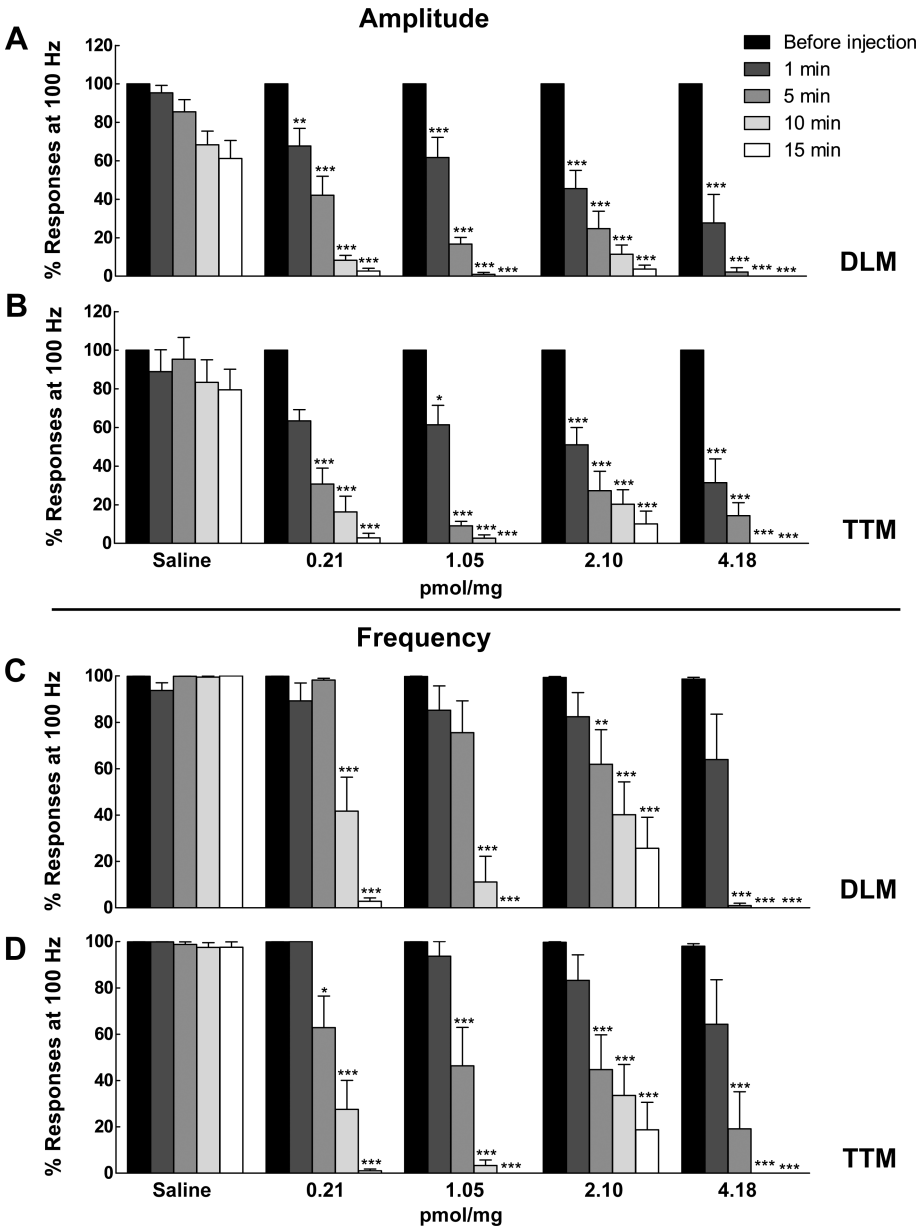

Figure 6. Effects of administration of Ap1a on the amplitude (top) and frequency (bottom) of responses from GF-DLM (A and C) and GF-TTM (B and D) pathways with increasing peptide doses (0.21, 1.05, 2.10, and 4.18 pmol/mg; $n = 8 \pm 2$ each). Both pathways were tested with 10 sweeps of 10 stimulus trains at 100 Hz before injection of saline or doses, and 1, 5, 10, and 15 min later. Data are presented as means ± the standard error of the mean using two-way ANOVA followed by a Bonferroni post-test. *$p < 0.05$, **$p < 0.01$, and ***$p < 0.001$ compared to control values.

time, $F_{(4, 21)} = 160.5$; interaction, $F_{(16, 205)} = 5.493$] and GF-TTM [dose, $F_{(4, 42)} = 52.48$; time, $F_{(4, 21)} = 94.37$; interaction, $F_{(16, 205)} = 4.939$]. Although there was also a reduction in amplitude in the control group responses over this time, the Ap1a-induced amplitude decrease was statistically significant at all peptide doses in GF-DLM and GF-TTM pathways in relation to the equivalent time in the control group. Only the smallest dose (0.21 pmol/mg) did not show a significant response in the GF-TTM pathway between the periods before and immediately after injection (1 min). Nevertheless, the subsequent intervals had significant responses, with $p < 0.001$ (Figure 6B).

Statistical analysis of the frequency of responses of both GF-DLM and GF-TTM pathways (Figure 6C,D) subjected to increasing doses of peptide also indicated significant differences between doses, times, and dose−time interactions with $p < 0.001$ for GF-DLM [dose, $F_{(4, 42)} = 32.39$; time, $F_{(4, 21)} = 57.66$; interaction, $F_{(16, 204)} = 6.858$] and GF-TTM [dose, $F_{(4, 42)} = 33.44$; time, $F_{(4, 21)} = 68.05$; interaction, $F_{(16, 205)} = 5.292$]. While in the control group the frequency of responses remained constant throughout the experiment (98.6 ± 2.7% for DLM and 98.7 ± 1.2% for TTM), significant reductions were observed in the GF-DLM pathway responses 10 and 15 min after injection of all peptide doses (Figure 6C), with $p < 0.001$, and also 5 min after injection of the largest doses, 2.10 and 4.18 pmol/mg, with $p < 0.01$ and $p < 0.001$, respectively. In the GF-TTM pathway (Figure 6D), there was a significant reduction in the frequency of responses at all assayed doses 5, 10, and 15 min after peptide injection.

At the largest peptide dose, there was no further response to stimuli in either pathway 5 min after peptide administration. On the other hand, the smallest dose induced a weaker effect,

dx.doi.org/10.1021/bi4000035 | *Biochemistry* 2013, 52, 2440−2452

which can be observed by the significance of both frequency and amplitude reduction responses. Thoracic stimuli, generated by electrode stimulation into the anterior end of the fly thorax, which directly stimulated the motor neurons, did not induce any effect at doses 0.21 and 4.18 pmol/mg at the end of the 15 min experimental protocol.

Therefore, Ap1a affects in a dose-dependent manner both the frequency and amplitude of GF-DLM and GF-TTM pathways' responses to brain stimulation in the *D. melanogaster* GF circuit.

Toxicity Assay in Mice. Ap1a (30 μg/animal) induced increased levels of urination, myoclonus, hypermotility with circular movements and jumps (starting 10 min after peptide injection), and generalized seizures (starting at 12 min) in mice. The tonic seizures were continuously repeated until the end of the experiment, characterizing the *status epilepticus*. Additionally, there was also tail hyperextension. The animals died between 25 and 35 min by respiratory failure because of generalized tonic seizures.

In Vitro Assays. The Ap1a peptide at 1 μM did not block or modulate the kinetics of nicotine receptors in the rhabdomyosarcoma cell preparation (Figure S5 of the Supporting Information). The response induced by addition of ACh was normal. As expected, α-bungarotoxin (0.1 μM) inhibited currents mediated by nicotinic receptors.

In electrophysiological experiments performed on $hNa_v1.2$, $hNa_v1.4$, $hNa_v1.5$, and $hNa_v1.6$ channels expressed in HEK cells (Figure S6 of the Supporting Information), Ap1a had no significant effect on the sodium peak current at a concentration of 1 μM.

DISCUSSION

This communication reports the chemical and biological characterization of Ap1a, the most abundant peptide in the venom of *A. paulensis*, noting that the major chromatographic fractions eluting before 45 min (35% acetonitrile) are low-molecular mass compounds, mainly acylpolyamines, as previously described.[13] Similar to those of many peptides from spider venoms that modulate ion channels,[12] the primary structure of Ap1a has a high content (29%) of basic amino acid residues, mainly Lys, and has a basic character (theoretical isoelectric point of 9.3).

There is a high degree of homology between the signal peptide and pro-peptide segments of Ap1a and the precursor sequences from *Lasiodora* sp., which also belongs to the Theraphosinae subfamily and, similar to *A. paulensis*, is found in Brazil, indicating an evolutionary proximity between these species.[25] Other precursor sequences that are homologous with Ap1a were found in the spiders *C. jingzhao* and *H. schmidti*, both found in China and from distinct subfamilies, Selenocosmiinae and Ornithoctoninae, respectively.[26,27]

The mature Ap1a sequence was 60−84% identical with those of spider toxins belonging to the HWTX-II family. U1-TRTX-Bs1a (TxP1), from *Brachypelma smithi* spider venom,[28] has 39 amino acid residues and is identical to U1-TRTX-Asp1b (ESTx2), from *Aphonopelma californicum* venom.[29] Together with U1-TRTX-Asp1a (ESTx1),[29] these three peptides have not had their biological activity described. U1-TRTX-Ba1a (Ba1) and U1-TRTX-Ba1b (Ba2), from the venom of the spider *Brachypelma ruhnaui* (*B. albiceps*), also have 39 amino acid residues and are toxic only to insects.[30] Like Ap1a, these five peptides have three disulfide bonds. The LpTxs (U1-TRTX-Lp1a and U1-TRTX-Lp1b), from *Lasiodora parahybana* venom, are longer peptides, such as Ap1a; however, unlike the others, they have four disulfide bonds. Both LpTxs were toxic to mice, but not to insects.[31]

HWTX-II, with 37 amino acid residues and three disulfide bonds,[32] has a paralytic dose-dependent activity on cockroaches (ED_{50} = 127 ± 54 μg/g) and blocks neuromuscular transmission in an isolated mouse phrenic nerve diaphragm preparation.[32] This last activity is also shared by both HWTX-VII and HWTX-VIII, which are also lethal to mice and induce paralysis in locusts.[27] Similarly, Ap1a is toxic to both insects and mice, although it has a higher potency in the latter. Ap1a has a considerably smaller paralytic dose on insects (ED_{50} = 13.01 ± 4.21 μg/g) than HWTX-II, even though different biological models were used. By way of contrast, toxins U1-TRTX-Ba1a and U1-TRTX-Ba1b were lethal to crickets (*Acheta domesticus*) with LD_{50} values of 10.8 ± 1.4 and 9.2 ± 0.9 μg/g, respectively, within 15 min of observation after injection.[30]

Unlike most spider toxins described to date, HWTX-II presents a different scaffold.[9] Its three-dimensional structure consists of two β-turns (Cys4−Ser7 and Lys24−Trp27) and a double-stranded antiparallel β-sheet (Trp27−Cys29 and Cys34−Lys36), lacking the characteristic cysteine knot of the ICK motif.[10] As for HWTX-II, structural analysis of U1-TRTX-Ba1b revealed that its cysteine connectivities are also consistent with the DDH motif. However, their three-dimensional structures cannot be superimposed.[30]

Here we show that Ap1a presents cystine linkages similar to those of toxin U1-TRTX-Bs1a (C_I−C_{IV}, C_{II}−C_V, and C_{III}−C_{VI}),[28] and to many other spider toxins.[4,6,33] However, unlike the consensus sequence of the ICK motif, Ap1a has a C_IX_3-$C_{II}X_{13}$-$C_{III}X_{11}$-$C_{IV}X_5$-C_VX_4-C_{VI} sequence, with larger segments between C_{II} and C_{III} and between C_{III} and C_{IV}. Moreover, in toxins that adopt the ICK motif, C_{III} and C_{IV} are usually vicinal,[4,6,12] which is not the case for Ap1a and U1-TRTX-Bs1a. Therefore, although these toxins have the same cysteine pairing as the ICK motif, this does not necessarily mean that they adopt the same tertiary structure. Other toxins whose primary structures resemble the ICK motif may lack the cysteine knot.[4] Given its disulfide bond pairing and predicted secondary structure, Ap1a probably contains a double-stranded β-sheet that seems to connect the N-terminal portion to the C-terminal portion of the peptide. Nevertheless, further structural analyses by either X-ray crystallography or nuclear magnetic resonance will be needed to assess the structure of Ap1a.

Despite the high levels of sequence identity among peptides from the HWTX-II family, Ap1a possesses two additional segments, one formed by residues Asp13−Lys17, in the long loop between C_{II} and C_{III}, and the other formed by residues Asp27−Lys30, between C_{III} and C_{IV}. Although not identical, this second segment is similar to that of LpTxs (21-CKCXDKDNKD-32). It was suggested that the LpTxs could adopt the DDH motif, modified by this extra segment that contains an additional disulfide bond.[11,12] However, because of the different biological activity of the LpTxs compared to those of other toxins of this family[31] and because of the lack of information about the connectivity of their cysteines or tertiary structures, it is still early to generate conclusions about their structural motifs.[12]

To attempt to identify the molecular target responsible for the insecticidal activity of Ap1a, we evaluated its effect in the *D. melanogaster* giant fiber (GF) circuit (Figure 5A). The GAP junctions present in the electrical synapses GF-TTMn and GF-PSI are dependent on the *Drosophila shaking-B* gene,[34] which

dx.doi.org/10.1021/bi4000035 | *Biochemistry* 2013, 52, 2440−2452

encodes transmembrane proteins that are analogous to connexins, the structural components of vertebrate gap junctions.[35−37] No arthropod toxins with activity on these synapses have been described.

The PSI-DLMn synapses are cholinergic,[38] mediated by nicotinic cholinergic receptor (nAChR) Dα7.[39] In mutant flies for *Dα7*, failures occurred in the DLM record after GF stimulation at 1, 10, and 100 Hz, and there was no response in the mutant allele with a more pronounced phenotype. This effect was explained by defects in the PSI-DLMn synapses identified by two observations. (i) The TTMs were able to properly follow giant fiber stimulation at 100 Hz at all mutant alleles, and (ii) possible defects in the DLM neuromuscular junctions were discarded, because direct stimulation of the DLMn through electrodes located in the thoracic cavity led to DLM records without failures at 100 Hz.[39]

Besides the electrical component, it has been shown that the GF-PSI and GF-TTMn synapses also have a chemical component. Nevertheless, different from the GF-TTMn pathway, it seems that the chemical component of the GF-PSI synapse is unable to function on its own.[40−42] Both NMJs of TTM and DLM are chemical synapses, with glutamate as the main neurotransmitter.[43] The neuromuscular glutamatergic synapses of *Drosophila* express postsynaptic receptors that are homologous to the non-NMDA receptors of vertebrates.[44−47]

Thus, if the PSI-DLMn synapse were the target of the Ap1a toxin, the response would be restricted to this pathway, because with its blockade, the TTM retained their responses to GF stimulation.[39] However, in the presence of Ap1a, there was a decrease in the amplitude and frequency in both pathways (GF-TTM and GF-DLM). Furthermore, Ap1a-treated flies were unresponsive to thoracic stimuli. This could indicate that Ap1a action is restricted to the NMJs of the GF circuit (TTMn-TTM and DLMn-DLM). The lack of an effect on cholinergic receptors can be further corroborated by two other results. (i) In the rhabdomyosarcoma cell preparation, Ap1a (1.0 μM) did not alter the response induced by ACh. (ii) In the frog isolated ventricle strip assay previously performed with *A. paulensis* venom fractions,[13] the protein fraction (35−74% acetonitrile), which contains Ap1a as the most abundant compound, presented effects different from those obtained through vagal stimulation.

The unusual shape of the TTM recording, with two adjacent peaks (Figure 5B), is possibly caused by the microelectrode not recording from a single muscle cell, which is more common in TTM recordings because of the many small fibers of this muscle, which makes it more difficult to maintain the position of the electrode after several muscle contractions. However, data are not affected, because the response latencies and frequency of following are preserved during the experiment.[48]

To verify if Ap1a was toxic to mammalians, 30 μg of peptide was injected into mice. Among the effects, the animals presented *status epilepticus* (SE), which is defined as continuous and persistent seizures (>5 min), or a series of two or more sequential seizures without full recovery of consciousness between them.[49,50] The SE is thought to result from a failure of the mechanisms that normally terminate an isolated seizure. This failure could be due to an abnormal persistence of excessive excitation or ineffective recruitment of inhibition. The proposed mechanisms of SE are constant activation of the hippocampus, loss of GABA-mediated inhibitory synaptic transmission in the hippocampus, and glutamatergic excitatory synaptic transmission, which is important for sustaining SE.[49]

To obtain an experimental model of SE, animals are often subjected to chemical agents or to electrical stimuli in the hippocampus or amygdala until *status epilepticus* has been reached.[51,52] Similar to Ap1a-treated mice, mice treated with intracerebroventricular injections of NMDA develop seizures through a sequence that includes bouts of itching, hypermotility and circular movements, jumps, involuntary muscle contractions of the forepaws, hypertonic tail, tonic-clonic seizures, *status epilepticus*, and eventually death.[53−55] It was observed that at doses of ∼10 mM NMDA, the generalized seizures occur 5−6 min after injection, with 75% mortality after severe tonic seizures.[54] This time is closer to the initial time of generalized seizures induced by Ap1a (12 min), if compared to that of kainic acid (KA)-induced seizures, which might take up to 2 h to display a full *status epilepticus*, despite different symptoms.[56−58] This suggests an action on glutamatergic neurotransmission, possibly by direct interaction of Ap1a with these receptors. However, glutamate receptors in the NMJs of the *Drosophila* GF circuit are not related to vertebrate NMDA receptors.[44−47] It is possible that this effect in mice was due to the large tested dose. This dose was chosen on the basis of previous assays with toxins δ-CNTX-Pn1b, γ-CNTX-Pn1a, and δ-CNTX-Pn1a from the spider *Phoneutria nigriventer*, which were toxic to insects by possibly affecting glutamatergic neurotransmission, but showed no toxic effects in mice at a dose of 30 μg/animal.[59−61] In addition to this action caused by the large dose of Ap1a, there are reports of signs of involvement of AMPA receptors in the production of seizures induced by NMDA administration, which is evidence of the interaction of different glutamatergic receptors during seizure syndromes.[62]

In the electrophysiological experiments performed with $hNa_v1.2$, $hNa_v1.4$, $hNa_v1.5$, and $hNa_v1.6$ channels expressed in HEK cells, Ap1a (1 μM) presented no significant effect, indicating that these are not its main molecular targets. In a similar way, the insecticidal toxins U1-TRTX-Ba1a and U1-TRTX-Ba1b (1 μM) showed no effect on mammalian $Na_v1.2$ and $Na_v1.5$ channels expressed in *Xenopus laevis* oocytes and did not affect *para*/*TipE* insect sodium currents.[30]

Because the protein fraction from *A. paulensis* venom (which contains Ap1a) showed no effect on the frog isolated ventricle strip assay, as previously reported,[13] it is possible that none of its compounds act on vertebrate Ca_v channels or that Ap1a might act on other Ca^{2+} channel subtypes different from those present in frog myocytes. Thus, testing Ap1a in different subtypes of Ca_v channels could ascertain whether this toxin could affect Ca^{2+} channels present in the presynaptic NMJs of the *D. melanogaster* GF circuit, which in turn could affect glutamatergic neurotransmission.

Despite recent advances in understanding *status epilepticus*, much remains to be explored. Given its medical importance, the use of new agents for experimental models may be advantageous in the study of SE.[49] Therefore, we suggest further investigation of the SE-inducing activity of Ap1a, as it could be used as a pharmacological tool for experimental models of *status epilepticus*.

Because of the peculiarities of Ap1a toxin, having signal peptide, pro-peptide, and a size similar to that of LpTxs, in addition to two extra segments in its sequence, but with only three disulfide bonds, which are assigned in a sequential manner (C_I−C_{IV}, C_{II}−C_V, and C_{III}−C_{VI}), just as in the ICK motif, this toxin is a novel structural model for the study of the HWXT-II family of peptides. The current characterization of another toxin with an "unusual" cystine framework for a spider

dx.doi.org/10.1021/bi4000035 | *Biochemistry* 2013, 52, 2440−2452

toxin (in addition to U1-TRTX-Bs1a) can lead to further analyses to help understand which mechanisms lead to different cysteine linkages, and if there is an evolutionary explanation for this, since the ICK fold can be considered as a minor elaboration of a simpler ancestral fold, termed the DDH fold.[7,63]

■ ASSOCIATED CONTENT

Supporting Information

Ap1a sequence and its alignment with other sequences from Theraphosidae spiders (Figure S1), MS/MS sequencing of the fragments generated after digestion of Ap1a to determine their cysteine pairings (Figures S2−S4), and electrophysiological experiments performed with Ap1a on nACh receptors and sodium channels (Figures S5 and S6, respectively). This material is available free of charge via the Internet at http://pubs.acs.org.

■ AUTHOR INFORMATION

Corresponding Author

*Departamento de Ciências Fisiológicas, Instituto de Ciências Biológicas, Laboratório de Toxinologia, Universidade de Brasília, Brasília, DF 70910-900, Brazil. Phone: 55.61.31073106. Fax: 55.61.31073107. E-mail: efschwa@unb.br.

Funding

This research was supported by grants from CNPq (303003/2009-0, 490068/2009-0, and 564223/2010-7) to E.F.S., from DPP-UnB (06/2010) to C.B.F.M., from the National Institutes of Health (1R21NS066371-01) to F.M., and from the DGAPA-UNAM (IN204110) to L.D.P. (Dirección General de Asuntos del Personal Académico, UNAM) and a CAPES scholarship to C.B.F.M. C.B.F.M. and E.A.B. received scholarships from CNPq.

Notes

The authors declare no competing financial interest.

■ ACKNOWLEDGMENTS

We acknowledge Dr. Márcia Mortari and Thalita Camargos, from Laboratório de Toxinologia at Universidade de Brasília, for helping with the mice and insecticidal assays and Dr. Paulo Motta, from Laboratório de Aracnídeos at Universidade de Brasília, for identifying the spiders.

■ ABBREVIATIONS

GF, giant fiber; DLM, dorsal longitudinal muscle; TTM, tergotrochanteral muscle; PSI, peripherally synapsing interneuron.

■ REFERENCES

(1) Rash, L. D., and Hodgson, W. C. (2002) Pharmacology and biochemistry of spider venoms. *Toxicon 40*, 225−254.

(2) Platnick, N. I. (2013) The world spider catalog, version 13.5, *AMNH*, online at http://research.amnh.org/iz/spiders/catalog, DOI: 10.5531/db.iz.0001 (March 10).

(3) Herzig, V., Wood, D. L., Newell, F., Chaumeil, P. A., Kaas, Q., Binford, G. J., Nicholson, G. M., Gorse, D., and King, G. F. (2011) ArachnoServer 2.0, an updated online resource for spider toxin sequences and structures. *Nucleic Acids Res. 39*, D653−D657.

(4) Vassilevski, A. A., Kozlov, S. A., and Grishin, E. V. (2009) Molecular diversity of spider venom. *Biochemistry (Moscow, Russ. Fed.) 74*, 1505−1534.

(5) Craik, D. J., Daly, N. L., and Waine, C. (2001) The cystine knot motif in toxins and implications for drug design. *Toxicon 39*, 43−60.

(6) Norton, R. S., and Pallaghy, P. K. (1998) The cystine knot structure of ion channel toxins and related polypeptides. *Toxicon 36*, 1573−1583.

(7) Wang, X., Connor, M., Smith, R., Maciejewski, M. W., Howden, M. E., Nicholson, G. M., Christie, M. J., and King, G. F. (2000) Discovery and characterization of a family of insecticidal neurotoxins with a rare vicinal disulfide bridge. *Nat. Struct. Biol. 7*, 505−513.

(8) Yuan, C. H., He, Q. Y., Peng, K., Diao, J. B., Jiang, L. P., Tang, X., and Liang, S. P. (2008) Discovery of a distinct superfamily of Kunitz-type toxin (KTT) from tarantulas. *PLoS One 3*, e3414.

(9) Shu, Q., Huang, R., and Liang, S. (2001) Assignment of the disulfide bonds of huwentoxin-II by Edman degradation sequencing and stepwise thiol modification. *Eur. J. Biochem. 268*, 2301−2307.

(10) Shu, Q., Lu, S. Y., Gu, X. C., and Liang, S. P. (2002) The structure of spider toxin huwentoxin-II with unique disulfide linkage: Evidence for structural evolution. *Protein Sci. 11*, 245−252.

(11) Diego-García, E., Peigneur, S., Waelkens, E., Debaveye, S., and Tytgat, J. (2010) Venom components from *Citharischius crawshayi* spider (Family Theraphosidae): Exploring transcriptome, venomics, and function. *Cell. Mol. Life Sci. 67*, 2799−2813.

(12) Escoubas, P., and Rash, L. (2004) Tarantulas: Eight-legged pharmacists and combinatorial chemists. *Toxicon 43*, 555−574.

(13) Mourão, C. B. F., Oliveira, F. N., e Carvalho, A. C., Arenas, C. J., Duque, H. M., Gonçalves, J. C., Macêdo, J. K., Galante, P., Schwartz, C. A., Mortari, M. R., Almeida Santos, M. F., and Schwartz, E. F. (2013) Venomic and pharmacological activity of *Acanthoscurria paulensis* (Theraphosidae) spider venom. *Toxicon 61*, 129−138.

(14) Caliskan, F., García, B. I., Coronas, F. I., Batista, C. V., Zamudio, F. Z., and Possani, L. D. (2006) Characterization of venom components from the scorpion *Androctonus crassicauda* of Turkey: Peptides and genes. *Toxicon 48*, 12−22.

(15) Suckau, D., Resemann, A., Schuerenberg, M., Hufnagel, P., Franzen, J., and Holle, A. (2003) A novel MALDI LIFT-TOF/TOF mass spectrometer for proteomics. *Anal. Bioanal. Chem. 376*, 952−965.

(16) Larkin, M. A., Blackshields, G., Brown, N. P., Chenna, R., McGettigan, P. A., McWilliam, H., Valentin, F., Wallace, I. M., Wilm, A., Lopez, R., Thompson, J. D., Gibson, T. J., and Higgins, D. G. (2007) Clustal W and Clustal X version 2.0. *Bioinformatics 23*, 2947−2948.

(17) Guerrero-Vargas, J. A., Mourão, C. B. F., Quintero-Hernandez, V., Possani, L. D., and Schwartz, E. F. (2012) Identification and phylogenetic analysis of *Tityus pachyurus* and *Tityus obscurus* novel putative Na^+-channel scorpion toxins. *PLoS One 7*, e30478.

(18) Finney, D. J. (1971) *Probit analysis*, 3rd ed., Cambridge University Press, London.

(19) Mejia, M., Heghinian, M. D., Busch, A., Armishaw, C. J., Mari, F., and Godenschwege, T. A. (2010) A novel approach for *in vivo* screening of toxins using the *Drosophila* Giant Fiber circuit. *Toxicon 56*, 1398−1407.

(20) Allen, M. J., Godenschwege, T. A., Tanouye, M. A., and Phelan, P. (2006) Making an escape: Development and function of the *Drosophila* giant fibre system. *Semin. Cell Dev. Biol. 17*, 31−41.

(21) Gu, H., and O'Dowd, D. K. (2006) Cholinergic synaptic transmission in adult *Drosophila* Kenyon cells *in situ*. *J. Neurosci. 26*, 265−272.

(22) Olamendi-Portugal, T., Batista, C. V., Restano-Cassulini, R., Pando, V., Villa-Hernandez, O., Zavaleta-Martinez-Vargas, A., Salas-Arruz, M. C., Rodriguez de la Vega, R. C., Becerril, B., and Possani, L. D. (2008) Proteomic analysis of the venom from the fish eating coral snake *Micrurus surinamensis*: Novel toxins, their function and phylogeny. *Proteomics 8*, 1919−1932.

(23) Schiavon, E., Sacco, T., Cassulini, R. R., Gurrola, G., Tempia, F., Possani, L. D., and Wanke, E. (2006) Resurgent current and voltage sensor trapping enhanced activation by a β-scorpion toxin solely in $Na_v1.6$ channel. Significance in mice Purkinje neurons. *J. Biol. Chem. 281*, 20326−20337.

(24) Augustin, H., Allen, M. J., and Partridge, L. (2011) Electrophysiological recordings from the giant fiber pathway of *D. melanogaster*. *J. Visualized Exp. 47*, e2412.
(25) Motta, P. C., and Bertani, R. (2010) Registros de aranhas (Araneae: Araneidae, Theraphosidae) e escorpiões (Scorpiones) do Cerrado. In *Cerrado: Conhecimento quantitativo como subsídio para as ações de conservação* (Diniz, I. R., Marinho-Filho, J., Machado, R. B., and Cavalcanti, R. B., Eds.) pp 149−185, Thesaurus, Brasília, Brazil.
(26) Chen, J., Deng, M., He, Q., Meng, E., Jiang, L., Liao, Z., Rong, M., and Liang, S. (2008) Molecular diversity and evolution of cystine knot toxins of the tarantula *Chilobrachys jingzhao*. *Cell. Mol. Life Sci. 65*, 2431−2444.
(27) Liang, S. (2004) An overview of peptide toxins from the venom of the Chinese bird spider *Selenocosmia huwena* Wang [=*Ornithoctonus huwena* (Wang)]. *Toxicon 43*, 575−585.
(28) Kaiser, I. I., Griffin, P. R., Aird, S. D., Hudiburg, S., Shabanowitz, J., Francis, B., John, T. R., Hunt, D. F., and Odell, G. V. (1994) Primary structures of two proteins from the venom of the Mexican red knee tarantula (*Brachypelma smithii*). *Toxicon 32*, 1083−1093.
(29) Savel-Niemann, A. (1989) Tarantula (*Eurypelma californicum*) venom, a multicomponent system. *Biol. Chem. Hoppe-Seyler 370*, 485−498.
(30) Corzo, G., Bernard, C., Clement, H., Villegas, E., Bosmans, F., Tytgat, J., Possani, L. D., Darbon, H., and Alagon, A. (2009) Insecticidal peptides from the theraposid spider *Brachypelma albiceps*: An NMR-based model of Ba2. *Biochim. Biophys. Acta 1794*, 1190−1196.
(31) Escoubas, P., Célérier, M. L., Romi-Lebrun, R., and Nakajima, T. (1997) Two novel peptide neurotoxins from the venom on the tarantula *Lasiodora parahybana*. *Toxicon 35*, 805−806.
(32) Shu, Q., and Liang, S. P. (1999) Purification and characterization of huwentoxin-II, a neurotoxic peptide from the venom of the Chinese bird spider *Selenocosmia huwena*. *J. Pept. Res. 53*, 486−491.
(33) Ferrat, G., and Darbon, H. (2005) An overview of the three dimensional structure of short spider toxins. *Toxin Rev. 24*, 359−381.
(34) Phelan, P., Stebbings, L. A., Baines, R. A., Bacon, J. P., Davies, J. A., and Ford, C. (1998) *Drosophila* Shaking-B protein forms gap junctions in paired *Xenopus* oocytes. *Nature 391*, 181−184.
(35) Baranova, A., Ivanov, D., Petrash, N., Pestova, A., Skoblov, M., Kelmanson, I., Shagin, D., Nazarenko, S., Geraymovych, E., Litvin, O., Tiunova, A., Born, T. L., Usman, N., Staroverov, D., Lukyanov, S., and Panchin, Y. (2004) The mammalian pannexin family is homologous to the invertebrate innexin gap junction proteins. *Genomics 83*, 706−716.
(36) Panchin, Y., Kelmanson, I., Matz, M., Lukyanov, K., Usman, N., and Lukyanov, S. (2000) A ubiquitous family of putative gap junction molecules. *Curr. Biol. 10*, R473−R474.
(37) Phelan, P., Goulding, L. A., Tam, J. L., Allen, M. J., Dawber, R. J., Davies, J. A., and Bacon, J. P. (2008) Molecular mechanism of rectification at identified electrical synapses in the *Drosophila* giant fiber system. *Curr. Biol. 18*, 1955−1960.
(38) Gorczyca, M., and Hall, J. C. (1984) Identification of a cholinergic synapse in the giant fiber pathway of *Drosophila* using conditional mutations of acetylcholine synthesis. *J. Neurogenet. 1*, 289−313.
(39) Fayyazuddin, A., Zaheer, M. A., Hiesinger, P. R., and Bellen, H. J. (2006) The nicotinic acetylcholine receptor Da7 is required for an escape behavior in *Drosophila*. *PLoS Biol. 4*, e63.
(40) Allen, M. J., and Murphey, R. K. (2007) The chemical component of the mixed GF-TTMn synapse in *Drosophila melanogaster* uses acetylcholine as its neurotransmitter. *Eur. J. Neurosci. 26*, 439−445.
(41) Baird, D. H., Schalet, A. P., and Wyman, R. J. (1990) The Passover locus in *Drosophila melanogaster*: Complex complementation and different effects on the giant fiber neural pathway. *Genetics 126*, 1045−1059.
(42) Thomas, J. B., and Wyman, R. J. (1984) Mutations altering synaptic connectivity between identified neurons in *Drosophila*. *J. Neurosci. 4*, 530−538.
(43) Jan, L. Y., and Jan, Y. N. (1976) L-Glutamate as an excitatory transmitter at the *Drosophila* larval neuromuscular junction. *J. Physiol. 262*, 215−236.
(44) Marrus, S. B., Portman, S. L., Allen, M. J., Moffat, K. G., and DiAntonio, A. (2004) Differential localization of glutamate receptor subunits at the *Drosophila* neuromuscular junction. *J. Neurosci. 24*, 1406−1415.
(45) Petersen, S. A., Fetter, R. D., Noordermeer, J. N., Goodman, C. S., and DiAntonio, A. (1997) Genetic analysis of glutamate receptors in *Drosophila* reveals a retrograde signal regulating presynaptic transmitter release. *Neuron 19*, 1237−1248.
(46) Qin, G., Schwarz, T., Kittel, R. J., Schmid, A., Rasse, T. M., Kappei, D., Ponimaskin, E., Heckmann, M., and Sigrist, S. J. (2005) Four different subunits are essential for expressing the synaptic glutamate receptor at neuromuscular junctions of *Drosophila*. *J. Neurosci. 25*, 3209−3218.
(47) Schuster, C. M., Ultsch, A., Schloss, P., Cox, J. A., Schmitt, B., and Betz, H. (1991) Molecular cloning of an invertebrate glutamate receptor subunit expressed in *Drosophila* muscle. *Science 254*, 112−114.
(48) Allen, M. J., and Godenschwege, T. A. (2010) Electrophysiological recordings from the Drosophila giant fiber system (GFS). *Cold Spring Harb Protocols 2010*, 10.1101/pdb.prot5453.
(49) Nair, P. P., Kalita, J., and Misra, U. K. (2011) Status epilepticus: Why, what, and how. *J. Postgrad. Med. (Bombay) 57*, 242−252.
(50) Tejeiro, J., and Gómez Sereno, B. (2003) Status epilepticus. *Rev. Neurol. 36*, 661−679.
(51) Garcia Garcia, M. E., Garcia Morales, I., and Matías Guiu, J. (2010) Experimental models in epilepsy. *Neurologia 25*, 181−188.
(52) Raol, Y. H., and Brooks-Kayal, A. R. (2012) Experimental models of seizures and epilepsies. *Prog. Mol. Biol. Transl. Sci. 105*, 57−82.
(53) Antonov, S. M., Johnson, J. W., Lukomskaya, N. Y., Potapyeva, N. N., Gmiro, V. E., and Magazanik, L. G. (1995) Novel adamantane derivatives act as blockers of open ligand-gated channels and as anticonvulsants. *Mol. Pharmacol. 47*, 558−567.
(54) Chang-Mu, C., Jen-Kun, L., Shing-Hwa, L., and Shoei-Yn, L. S. (2010) Characterization of neurotoxic effects of NMDA and the novel neuroprotection by phytopolyphenols in mice. *Behav. Neurosci. 124*, 541−553.
(55) Marganella, C., Bruno, V., Matrisciano, F., Reale, C., Nicoletti, F., and Melchiorri, D. (2005) Comparative effects of levobupivacaine and racemic bupivacaine on excitotoxic neuronal death in culture and N-methyl-D-aspartate-induced seizures in mice. *Eur. J. Pharmacol. 518*, 111−115.
(56) Chuang, Y. C., Chang, A. Y., Lin, J. W., Hsu, S. P., and Chan, S. H. (2004) Mitochondrial dysfunction and ultrastructural damage in the hippocampus during kainic acid-induced status epilepticus in the rat. *Epilepsia 45*, 1202−1209.
(57) Mulle, C., Sailer, A., Perez-Otano, I., Dickinson-Anson, H., Castillo, P. E., Bureau, I., Maron, C., Gage, F. H., Mann, J. R., Bettler, B., and Heinemann, S. F. (1998) Altered synaptic physiology and reduced susceptibility to kainate-induced seizures in GluR6-deficient mice. *Nature 392*, 601−605.
(58) Zhang, X. M., and Zhu, J. (2011) Kainic acid-induced neurotoxicity: Targeting glial responses and glia-derived cytokines. *Curr. Neuropharmacol. 9*, 388−398.
(59) de Figueiredo, S. G., de Lima, M. E., Nascimento Cordeiro, M., Diniz, C. R., Patten, D., Halliwell, R. F., Gilroy, J., and Richardson, M. (2001) Purification and amino acid sequence of a highly insecticidal toxin from the venom of the brazilian spider *Phoneutria nigriventer* which inhibits NMDA-evoked currents in rat hippocampal neurones. *Toxicon 39*, 309−317.
(60) Oliveira, L. C., De Lima, M. E., Pimenta, A. M., Mansuelle, P., Rochat, H., Cordeiro, M. N., Richardson, M., and Figueiredo, S. G. (2003) PnTx4−3, a new insect toxin from *Phoneutria nigriventer* venom elicits the glutamate uptake inhibition exhibited by PhTx4 toxic fraction. *Toxicon 42*, 793−800.

(61) Figueiredo, S. G., Garcia, M. E., Valentim, A. C., Cordeiro, M. N., Diniz, C. R., and Richardson, M. (1995) Purification and amino acid sequence of the insecticidal neurotoxin Tx4(6−1) from the venom of the 'armed' spider *Phoneutria nigriventer* (Keyserling, 1891). *Toxicon 33*, 83−93.
(62) Lukomskaya, N. Y., Rukoyatkina, N. I., Gorbunova, L. V., Gmiro, V. E., and Magazanik, L. G. (2004) Studies of the roles of NMDA and AMPA glutamate receptors in the mechanism of corasole convulsions in mice. *Neurosci. Behav. Physiol. 34*, 783−789.
(63) Smith, J. J., Hill, J. M., Little, M. J., Nicholson, G. M., King, G. F., and Alewood, P. F. (2011) Unique scorpion toxin with a putative ancestral fold provides insight into evolution of the inhibitor cystine knot motif. *Proc. Natl. Acad. Sci. U.S.A. 108*, 10478−10483.